Pergamon

Geochimica et Cosmochimica Acta, Vol. 68, No. 19, pp. 3909-3918, 2004

0016-7037/04 $30.00 + .00

doi:10.1016/j.gca.2004.03.027

Ab initio calculation of ^{1}H, ^{17}O, ^{27}Al and ^{29}Si NMR parameters, vibrational frequencies and bonding energetics in hydrous silica and Na-aluminosilicate glasses

J. D. KUBICKI[1,*] and D. G. SYKES[2]

[1]Department of Geosciences, The Pennsylvania State University, University Park, PA 16802, USA
[2]Department of Chemistry, The Pennsylvania State University, University Park, PA 16802, USA

(*Received August* 14, 2003; *accepted in revised form March* 31, 2004)

Abstract—Ab initio, molecular orbital (MO) calculations were performed on model systems of SiO_2, $NaAlSi_3O_8$ (albite), H_2O-SiO_2 and H_2O-$NaAlSi_3O_8$ glasses. Model nuclear magnetic resonance (NMR) isotropic chemical shifts (δ_{iso}) for ^{1}H, ^{17}O, ^{27}Al and ^{29}Si are consistent with experimental data for the SiO_2, $NaAlSi_3O_8$, H_2O-SiO_2 systems where structural interpretations of the NMR peak assignments are accepted. For H_2O-$NaSi_3AlO_8$ glass, controversy has surrounded the interpretation of NMR and infrared (IR) spectra. Calculated δ_{iso} ^{1}H, δ_{iso} ^{17}O, δ_{iso} ^{27}Al and δ_{iso} ^{29}Si are consistent with the interpretation of Kohn et al. (1992) that Si-(OH)-Al linkages are responsible for the observed peaks in hydrous Na-aluminosilicate glasses. In addition, a theoretical vibrational frequency associated with the Kohn et al. (1992) model agrees well with the observed shoulder near 900 cm^{-1} in the IR and Raman spectra of hydrous albite glasses. MO calculations suggest that breaking this Si-(OH)-Al linkage requires ~+56 to +82 kJ/mol which is comparable to the activation energies for viscous flow in hydrous aluminosilicate melts. *Copyright © 2004 Elsevier Ltd*

1. INTRODUCTION

Dissolution of water into Na-aluminosilicate melts is one of the most important reactions in geochemistry because this reaction plays a role in the formation of granitic magmas. Furthermore, the reverse reaction, or exsolution, is important in pyroclastic eruptions. For many years, this reaction was believed to occur via hydrolysis of T-O-T linkages where T is a tetrahedral Si or Al cation (e.g., Burnham, 1979; Mysen and Virgo, 1986). In contrast, NMR investigations proposed the formation of T-(OH)-T linkages without hydrolysis of the melt (Kohn et al., 1989, 1992; Kohn, 2000; Schmidt et al., 2000). Earlier work (Sykes and Kubicki, 1993; Sykes et al., 1997) addressed both the vibrational and NMR spectra of hydrous Na-aluminosilicate glasses. Based on agreement between calculated ^{27}Al NMR parameters in Q^3 Al-(OH) model clusters and experimental NMR spectra of hydrous albite glass, we supported the interpretation of network depolymerization to form terminal T-OH groups. More recent ^{17}O NMR investigations have suggested a more complicated solubility mechanism involving the formation of T-(OH)-T linkages with some evidence for Si-OH species (Xu et al., 1998; Oglesby and Stebbins, 2000; Schmidt et al., 2000). A similar conclusion was derived via an ab initio modeling study by Liu et al. (2002).

There are two main improvements included in this paper over our past models. The first is that ^{17}O NMR spectra of hydrous silicate gels and glasses are now available (e.g., Cong and Kirkpatrick, 1996; Dirken et al., 1997; Maekawa et al., 1998; Xu et al., 1998; van Eck et al., 1999; Lee and Stebbins, 2000) for comparison to model calculations. A complication in each of our earlier investigations was that the proposed mechanisms were based on an analysis of the spectroscopic data of nuclei (i.e., Si and Al) not directly involved in the solubility mechanism. Oxygen sites in fully polymerized Na-aluminosilicate melts are the sites of either protonation or hydrolysis, so an analysis of the oxygen sites should be a more sensitive probe of the water solubility mechanism. The second improvement is that the effects of H-bonding to molecular water are included in our model clusters. H-bonding in molecular models significantly affects calculated ^{17}O NMR parameters (Xue and Kanzaki, 1998, 1999); hence, inclusion of H-bonding effects is important in obtaining accurate results.

2. METHODS

Molecular clusters were optimized with HF/3-21G(d,p) basis sets in Gaussian 98 (Frisch et al., 1998). These energy-minimized structures were subjected to force constant analyses to obtain vibrational frequencies. A scaling factor of 0.89 (Pople et al., 1981) was used to compare theoretical and experimental vibrational frequencies. All model clusters were OH-terminated, but we use a shorthand notation for their description. For example, the Q^4 Si model cluster $([OH_3]SiO)_4Si$ is denoted as $(Si_4)Si$ (Table 1).

Isotropic NMR chemical shifts, δ_{iso}, and quadrupolar coupling constants, C_q, were calculated based on these structures. (Note that experimental NMR chemical shifts are not always reported as isotropic values. We have endeavored to find isotropic chemical shifts wherever possible, and we report non-isotropic chemical shifts for ^{17}O and ^{27}Al as "peak maxima.") ^{1}H and ^{29}Si values were computed with HF/6-311+G(d,p) basis sets, ^{27}Al with HF/6-31G(d), and ^{17}O values were computed with the B3LYP/6-311+G(d,p) method. This latter hybrid MO/DFT method has been shown to be more accurate than Hartree-Fock methods for ^{17}O NMR parameters in aluminosilicates (Casanovas et al., 1999; Kubicki and Toplis, 2002). Calculated isotropic chemical shift values were based on the difference in theoretical chemical shieldings of model molecules and model standards. These model standards were constructed to mimic the experimental standards. We used a 19 H_2O cluster for ^{17}O, $Al^{3+} \cdot 6(H_2O)$ for ^{27}Al, and tetramethylsilane (TMS) for ^{1}H and ^{29}Si. The value of the ^{17}O chemical shielding used for the chemical shift calculations was obtained by averaging the chemical shieldings of all nineteen oxygens in the 19 H_2O model standard.

Quadrupolar coupling constants (C_q) were calculated using $C_q = eq_{zz}eQ$ where eQ is the nuclear electric quadrupole moment of the nucleus and all other terms are the principal tensor components of the electric field gradient. The values of the nuclear electric quadrupole

* Author to whom correspondence should be addressed (kubicki@geosc.psu.edu).

Table 1. Notation used for the clusters included in this study.

Glass	Notation	Formula
Silica	$(Si_4)Si$	$[((OH)_3SiO)_4Si]$
	$(Si_{17})Si$	$[((H_3SiO)_3SiO)_4Si]$
Albite	$Na^+[(Si_3Al)Si]$	$Na^+[((OH)_3SiO)_3(OH)_3AlOSi]$
	$Na^+[(Si_4)Al]$	$Na^+[((OH)_3SiO)_4Al]$
Hydrous silica	$(Si_3)SiOH$	$[((OH)_3SiO)_3SiOH]$
	$(Si_3)SiOH + 2H_2O$	$[((OH)_3SiO)_3SiOH] \cdot 2H_2O$
	$H^+(Si_4)Si$	$H^+[((OH)_3SiO)_4Si]$
	$H^+(Si_4)Si + H_2O$	$H^+[((OH)_3SiO)_4Si] \cdot H_2O$
Hydrous albite	$Na^+(Si_2Al)SiOH$	$Na^+[((OH)_3SiO)_2(OH)_3AlOSiOH]$
	$Na^+(Si_2Al)SiOH + 2H_2O$	$Na^+[((OH)_3SiO)_2(OH)_3AlOSiOH] \cdot 2H_2O$
	$H^+(Si_3Al)Si$	$H^+[((OH)_3SiO)_3(OH)_3AlOSi]$
	$H^+(Si_3Al)Si + H_2O$	$H^+[((OH)_3SiO)_3(OH)_3AlOSi] \cdot H_2O$
	$Na^+(Si_3)AlOH$	$Na^+[((OH)_3SiO)_3AlOH]$
	$Na^+(Si_3)AlOH + 2H_2O$	$Na^+[((OH)_3SiO)_3AlOH] \cdot 2H_2O$
	$H^+(Si_4)Al$	$H^+[((OH)_3SiO)_4Al]$
	$H^+(Si_4)Al + H_2O$	$H^+[((OH)_3SiO)_4Al] \cdot H_2O$

moments were obtained from Pyykkö (1992). Accuracy of the computed NMR parameters was tested on models representing commonly accepted structures in anhydrous silica and albite glasses as well as hydrous silica glass. Furthermore, the cluster size effect on calculated chemical shifts has been tested in Kubicki and Toplis (2002) and shown to be within errors generated by limited basis sets and neglect of electron correlation.

Reaction paths for breaking an Si-(OH)-Al linkages were determined by constrained optimizations (Felipe et al., 2001) using the HF/3-21G(d,p) basis set. Energies at each point along the reaction path were obtained with the B3LYP/6-311+G(d,p) basis set.

3. RESULTS

3.1. Accuracy Tests Against Anhydrous Silica Glass Spectra

The cluster $(Si_4)Si$ was used to represent Si and O in anhydrous silica glass. The central Si is fully-polymerized (i.e., Q^4 where the $Q^{\#}$ represents the number of bridging oxygen atoms attached to a tetrahedral cation) in this model as it is in the glass, and the bridging oxygen atoms have the same atoms surrounding them out to second-nearest neighbor distances. Experimental and calculated $\delta_{iso}{}^{29}Si$ values are both −112 ppm (Table 2), which is fortuitously accurate agreement because more accurate basis sets used for energy minimization and chemical shieldings can give less accurate agreement (Sykes et al., 1997).

Computed $\delta_{iso}{}^{17}O$ values range from 37 to 55 ppm (Table 3), which coincides with the *observed* peak maximum centered at ~50 ppm in silica gel (Walter et al., 1988) and similar to isotropic $\delta^{17}O$ values which range from 29 to 58 ppm for the quartz polymorph, coesite (Grandinetti et al., 1995). We report several values of $\delta_{iso}{}^{17}O$ for each model cluster (Table 3) as each oxygen atom within a cluster has a slightly different chemical environment, giving rise to different values of $\delta_{iso}{}^{17}O$, consistent with experimental observations (Grandinetti et al., 1995). The C_q value for ^{17}O is 5.8 MHz in silica (Walter et al., 1988), between 5 and 6 MHz in coesite (Grandinetti et al., 1995), and our calculated average value is 6.6 MHz.

3.2. Accuracy Tests Against Anhydrous Albite Glass Spectra

A number of models consisting of five tetrahedra (i.e., Q^4 Si and Al) with various numbers of Si and Al cations charge-

Table 2. Calculated $\delta_{iso}{}^{29}Si$ values based on HF/6-311+G(d,p) calculations with $Si(CH_3)_4$ (TMS) as the reference with a theoretical chemical shieldings of 397 ppm (Sykes et al., 1997).

Glass	Model	Species	Expt	Calc
Silica	$(Si_4)Si$	Si (Q^4)	–112[a]	–112
Albite	$Na^+[(Si_3Al)Si]$	Si (Q^4)	–99[b]	–95
Hydrous silica			–100[c]	
	$(Si_3)SiOH$	Si (Q^3 SiOH)		–98
	$(Si_3)SiOH + 2H_2O$	Si (Q^3 SiOH)		–100
	H^+ $(Si_4)Si$	Si (Q^4 Si)		–105
	$H^+(Si_4)Si + H_2O$	Si (Q^4)		–104
Hydrous albite			–98.3[d]	
	$Na^+(Si_2Al)SiOH$	Si (Q^3 SiOH)		–96
	$Na^+(Si_2Al)SiOH + 2H_2O$	Si (Q^3 SiOH)		–91
	$H^+(Si_3Al)Si$	Si (Q^4)		–95
	$H^+(Si_3Al)Si + H_2O$	Si (Q^4)		–97

[a] Murdoch et al. (1985).
[b] Oestrike et al (1987).
[c] Farnan et al. (1987).
[d] Kohn et al. (1992).

Table 3. Calculated δ_{iso} ^{17}O values based on B3LYP/6-311+G(d,p) basis sets and a reference cluster of $(H_2O)_{19}$ with an average oxygen chemical shielding of 293 ppm. T-O-T angles (in degrees) are listed in parentheses.

Glass	Model	Species	Expt	Calc
Silica			≈50[a]	
	$(Si_4)Si$	O_{br} (SiOSi)		55 (151)
				49 (154)
				46 (156)
				37 (173)
	$(Si_{17})Si$	O_{br} (SiOSi)	≈50[a]	49 (142)
Albite		SiOSi	48[b]	
		SiOAl	34[b]	
	$Na^+[(Si_3Al)Si]$	O_{br} (SiOSi)		54 (130)
				59 (171)
				54 (139)
	$Na^+[(Si_3Al)Si]$	O_{br} (SiOAl)		38 (149)
	$Na^+[(Si_4)Al]$	O_{br} (SiOAl)		42 (126)
				39 (127)
				57 (158)
				39 (140)
Hydrous silica		SiOSi	37[c]–42[d]	
		SiOH	37[e]	
	$(Si_3)SiOH$	O_{br} (SiOSi)		44 (143)
				55 (152)
				60 (146)
	$(Si_3)SiOH$	O (Q^3 SiOH)		6
	$(Si_3)SiOH + 2H_2O$	O_{br} (SiOSi)		39 (165)
				59 (148)
				56 (147)
	$(Si_3)SiOH + 2H_2O$	O (Q^3 SiOH)		33
	H^+ $(Si_4)Si$	O_{br} (SiOSi)		44 (142)
				42 (157)
				44 (161)
	$H^+(Si_4)Si$	O (SiOHSi)		60 (125)
	$H^+(Si_4)Si + H_2O$	O_{br}(SiOSi)		45 (141)
				50 (156)
				46 (162)
	$H^+(Si_4)Si + H_2O$	O_{br}(SiOHSi)		69 (126)
Hydrous albite		SiOSi	43[f]	
		SiOAl	33[f]	
		SiOHAl or TOH	≈48[g]	
	$Na^+(Si_2Al)SiOH$	O_{br} (SiOSi)		53 (154)
				45 (162)
	$Na^+(Si_2Al)SiOH$	O_{br} (SiOAl)		38 (141)
	$Na^+(Si_2Al)SiOH$	O (OH)		4
	$Na^+(Si_2Al)SiOH + 2H_2O$	O_{br}(SiOSi)		54 (141)
				46 (163)
	$Na^+(Si_2Al)SiOH + 2H_2O$	O_{br}(SiOAl)		40 (151)
	$Na^+(Si_2Al)SiOH + 2H_2O$	O (Q^3 SiOH)		28
	$Na^+(Si_3)AlOH$	O_{br} (SiOAl)		36 (132)
				37 (154)
				27 (157)
	$Na^+(Si_3)AlOH$	O (Q^3 AlOH)		–18
	$Na^+(Si_3)AlOH + 2H_2O$	O_{br} (SiOAl)		36 (130)
				46 (165)
				43 (130)
	$Na^+(Si_3)AlOH + 2H_2O$	O (Q^3 AlOH)		5
	$H^+(Si_4)Al$	O_{br}(SiOAl)		31 (134)
				61 (151)
				41 (140)
	$H^+(Si_4)Al$	O_{br} (SiOHAl)		24 (115)
	$H^+(Si_4)Al + H_2O$	O_{br} (SiOAl)		30 (137)
				66 (150)
				42 (140)
	$H^+(Si_4)Al + H_2O$	O_{br} (SiOHAl)		40 (114)
	$H^+(Si_3Al)Si$	O_{br} (SiOSi)		56 (127)
				58 (170)
				48 (142)
	$H^+(Si_3Al)Si$	O_{br} (SiOHAl)		35 (122)
	$H^+(Si_3Al)Si + H_2O$	O_{br} (SiOSi)		48 (141)
				63 (169)
				50 (144)
	$H^+(Si_3Al)Si + H_2O$	O_{br} (SiOHAl)		43 (119)

[a] Walter et al. (1988).
[b] Lee and Stebbins (2000).
[c] van Eck et al. (1999).
[d] Maekawa et al. (1998).
[e] Cong and Kirkpatrick (1996).
[f] Xu and Stebbins (1998) stilbite (Na,Ca)zeolite.
[g] Xu et al. (1998).

Table 4. Calculated δ_{iso} ^{27}Al values based on HF/6-31G(d) calculations with $Al^{3+} \cdot 6(H_2O)$ as the references with a theoretical chemical shielding of 633 ppm (Sykes et al., 1997).

Glass	Model	Species	Expt	Calc
Albite			57.5[a]	
Hydrous albite	$Na^+[(Si_4)Al]$	Al (Q^4)	53–54[b]	61
Hydrous albite	$Na^+(Si_3)AlOH$	Al (Q^3 AlOH)		57
	$Na^+(Si_3)AlOH + 2H_2O$	Al (Q^3 AlOH)		64
	$H^+(Si_4)Al$	Al (Q^4 Al)		57
	$H^+(Si_4)Al + H_2O$	Al (Q^4 Al)		56

[a] Schmidt et al. (2000).
[b] Kohn et al. (1992).

balanced with Na^+ were used to model albite glass. The experimental versus theoretical comparison for δ_{iso} ^{29}Si in this case gives −99 and −95 ppm, respectively (Table 2). For ^{27}Al, Schmidt et al. (2000) report a mean δ_{iso} ^{27}Al of 57.5 ppm for $NaAlSi_{4.7}O_{11.4}$ glass with ~3.8 wt.% water. These authors also observed that the mean δ_{iso} ^{27}Al for a series of hydrated glasses along the quartz-albite join became more positive with increasing Al-content. Our value of 61 ppm for $NaAlSi_3O_8$ (Table 4) is consistent with the results of Schmidt et al. (2000).

Best-fit simulations of experimental δ^{17}O MQMAS spectra assign δ_{iso} ^{17}O at 49 and 33 ppm to bridging oxygen atoms in Si-O-Si and Al-O-Si linkages, respectively (Dirken et al., 1997). Lee and Stebbins (2000) report similar δ_{iso} ^{17}O values (48 ppm for Si-O-Si and 34 ppm for Al-O-Si; Table 3). Our calculations predict δ_{iso} ^{17}O for Si-O-Si to range from 54 to 59 ppm and δ_{iso} ^{17}O for Al-O-Si to range from 38 to 57 ppm (Table 3). Experimentally-derived C_q values for the Si-O-Si and Si-O-Al oxygens are 5.1 and 3.5 MHz, respectively (Dirken et al., 1997); whereas our calculations result in values of 6.2 and 4.6 MHz, respectively.

The above model values agree fairly well with experimental values for each species in the anhydrous glasses. Either the calculated chemical shift value was in error by ≈5 to 10 ppm or the experimental and model ranges of values overlap. C_q values were systematically overestimated by ~1 MHz. The systematic error was due to small inaccuracies in calculated bond lengths and intertetrahedral angles (Clark and Grandinetti, 2003). However, the compositional trends are reproduced for both δ_{iso} ^{17}O and ^{17}O C_q values. We conclude that our methodology can produce reliable predictions for chemical shifts and C_q values in glasses because the errors are reasonably small and systematic (see also Liu et al., 2002).

3.3. Comparison of Model Results to Hydrous SiO_2 Glass Spectra

Agreement between experiment and theory for δ_{iso} ^{29}Si chemical shifts is excellent for the hydrous silica glass when the $(Si_3)SiOH$ model is used (−100 ppm experimental and −98 or −100 ppm calculated depending on the presence of H_2O molecules; Table 2). For these Q^3 SiOH molecules, we calculate δ_{iso} ^{17}O values of 39 to 60 ppm for bridging oxygens (Table 3) compared to δ_{iso} ^{17}O of 42 ppm from experiment (van Eck et al., 1999). A δ_{iso} ^{17}O at 37 ppm has been assigned to oxygen atoms in hydroxyl groups in a hydrated calcium silicate gel (Cong and Kirkpatrick, 1996), and our calculations predict 33 ppm when two H_2O molecules are H-bonded to the (Si)OH. H-bonding of the (Si)OH group to the molecular water is critical because without the extra H_2O, the δ_{iso} ^{17}O value is 6 ppm, which is not close to experiment (Table 3). H-bonding also affects the predicted δ_{iso} ^{1}H value as the $(Si_3)Si(OH)$ species has a value of 1.7 ppm and the $(Si_3)Si(OH) + 2H_2O$ cluster is calculated to be 7.9 ppm (Table 5). These changes in the ^{1}H-NMR chemical shifts are consistent with previous interpretations of experimental data (Zeng et al., 1999).

In models with Si-(OH)-Si linkages (with and without

Table 5. Calculated δ_{iso} ^{1}H values based on HF/6-311+G(d,p)/HF/3-21 G(d,p) calculations on TMS with $\sigma(^1H) = 32.5$ ppm.

Glass	Model	Species	Expt	Calc
Hydrous silica	$(Si_3)SiOH$	H (Q^3 SiOH)	1.7	1.7
	$(Si_3)SiOH + 2H_2O$	H (Q^3 SiOH)	5–6	7.9
	$H^+(Si_4)Si$	H (SiOHSi)	1.7[a]	12.3
	$H^+(Si_4)Si + H_2O$	H (SiOHSi)	5–6[b]	13.8
Hydrous albite	$Na^+(Si_2Al)SiOH$	H (Q^3 SiOH)	1.5	1.7
	$Na^+(Si_2Al)SiOH + 2H_2O$	H (Q^3 SiOH)	5–6	7.5
	$Na^+(Si_3)AlOH$	H (Q^3 AlOH)	3.5	0.1
	$Na^+(Si_3)AlOH + 2H_2O$	H (Q^3 AlOH)	5–6	1.7
	$H^+(Si_4)Al$	H (SiOHAl)	3.5[b]	3.3
	$H^+(Si_4)Al + H_2O$	H (SiOHAl)	3.8[b]	10.9
	$H^+(Si_3Al)Si$	H (SiOHAl)	5–6[c]	6.2
	$H^+(Si_3Al)Si + H_2O$	H (SiOHAl)	5–6[c]	12.2

[a] Chuang et al. (1993).
[b] Kohn et al. (1992).
[c] Zeng et al. (1999).

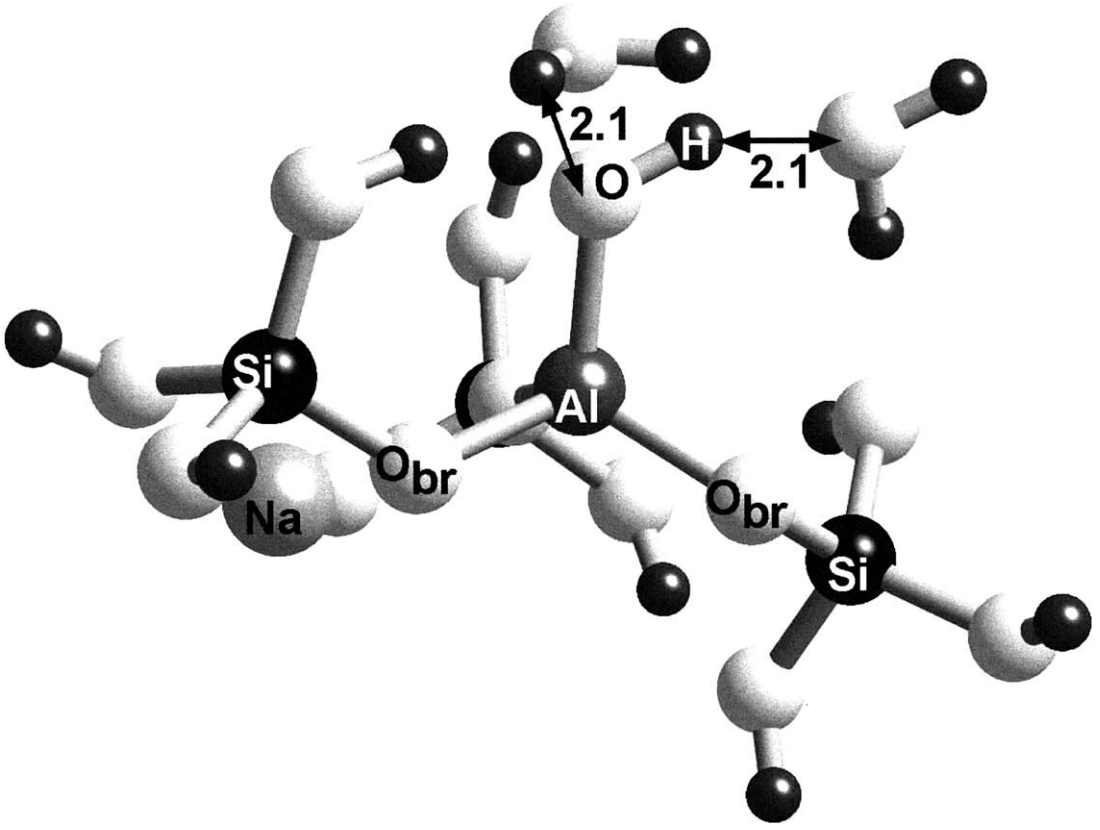

Fig. 1. Q^3 Al-OH species suggested by Sykes and Kubicki (1993) with H_2O molecules H-bonded at 2.1 Å to the hydroxyl group in Al-OH. Note that a variety of other Q^3 species (both Al and Si) were modeled in this study as well (Tables 1–4).

H-bonds to H_2O), $\delta_{iso}{}^{29}$Si is −104 and −105 ppm, respectively (Table 2). $\delta_{iso}{}^{17}$O values in bridging oxygen atoms were calculated to be 42 to 50 ppm, respectively, for these same model clusters. Hence, the O_{br} values in the $H^+(Si_4)Si$ models are similar to the $(Si_3)SiOH$ models. However, the $\delta_{iso}{}^{17}$O values for Si-(OH)-Si oxygen atoms were 60 and 69 ppm (Table 3), significantly higher than the $(Si_3)SiOH$ models and experiment. Model $\delta_{iso}{}^{1}$H in both the $H^+(Si_4)Si$ and $H^+(Si_4)Si + H_2O$ cluster were higher (12.3 and 13.8 ppm, respectively; Table 5) than observed in experiment (1.7 to 6 ppm).

Consistently better agreement was achieved for the model clusters based on $(Si_3)Si(OH)$ (i.e., hydrolysis) than $H^+(Si_4)Si$ (i.e., protonation). Consensus exists that the solvation mechanism of water in silica melt involves depolymerization and formation of Q^3 Si(OH) (Stolen and Walrafen, 1976). We conclude that our models and computational methods are reliable in predicting NMR chemical shifts in hydrous glasses as well as anhydrous glasses when the effects of H-bonding to molecular water are included.

3.4. Comparison of Model Results to Hydrous Albite Glass NMR Spectra

We compared our model hydrous albite glass δ^{17}O values to a related system, the zeolite stilbite, where Xu and Stebbins (1998) found δ^{17}O values of 43 and 33 ppm for oxygen atoms in SiOSi and SiOAl linkages, respectively. In addition, the $\delta_{iso}{}^{17}$O of oxygens in hydroxyl groups of hydrous albite glass have been assigned to a resonance at ≈48 ppm (Xu et al., 1998). Our calculated SiOH group is not close to this latter value in the $Na^+(Si_2Al)SiOH + 2H_2O$ cluster (28 ppm). The model AlOH group in $Na^+(Si_3)AlOH + 2H_2O$ (Fig. 1) produces a value that is even farther from observation at 5 ppm (Table 3). The agreement is worse if H-bonding is not included because the $Na^+(Si_3)AlOH$ cluster has a $\delta_{iso}{}^{17}$O value of −18 ppm for the oxygen in Al(OH).

Models representing the T-(OH)-T structure ($H^+[Si_4]Al + H_2O$ and $H^+[Si_3Al]Si + H_2O$; Figure 2) suggested by Kohn et al. (1992) result in calculated $\delta_{iso}{}^{17}$O values of 40 to 43 ppm, respectively (Table 3), much closer to the experimental values. Again, H-bonding plays a role in the calculated value of the $\delta_{iso}{}^{17}$O, but it is not as large as the Q^3 TOH case because the non-H-bonded values were shifted by −16 and −17 ppm, respectively (Table 3). In fact, in this case, the value calculated without H-bonding (for $H^+[Si_3Al]Si$ = 35 ppm) is in better agreement with experiment (observed = 33 ppm) than the clusters that included H-bonding to H_2O.

Both the Q^3 T-(OH) and T-(OH)-T models result in calculated $\delta_{iso}{}^{29}$Si and $\delta_{iso}{}^{27}$Al values reasonably close to experiment (Tables 1 and 4). However, in each case, the T-(OH)-T configuration gives somewhat better agreement. For example, the experimental isotropic ^{27}Al chemical shift is 54 ppm; the T-(OH)-T configuration is 56 or 57 ppm whereas the T-OH

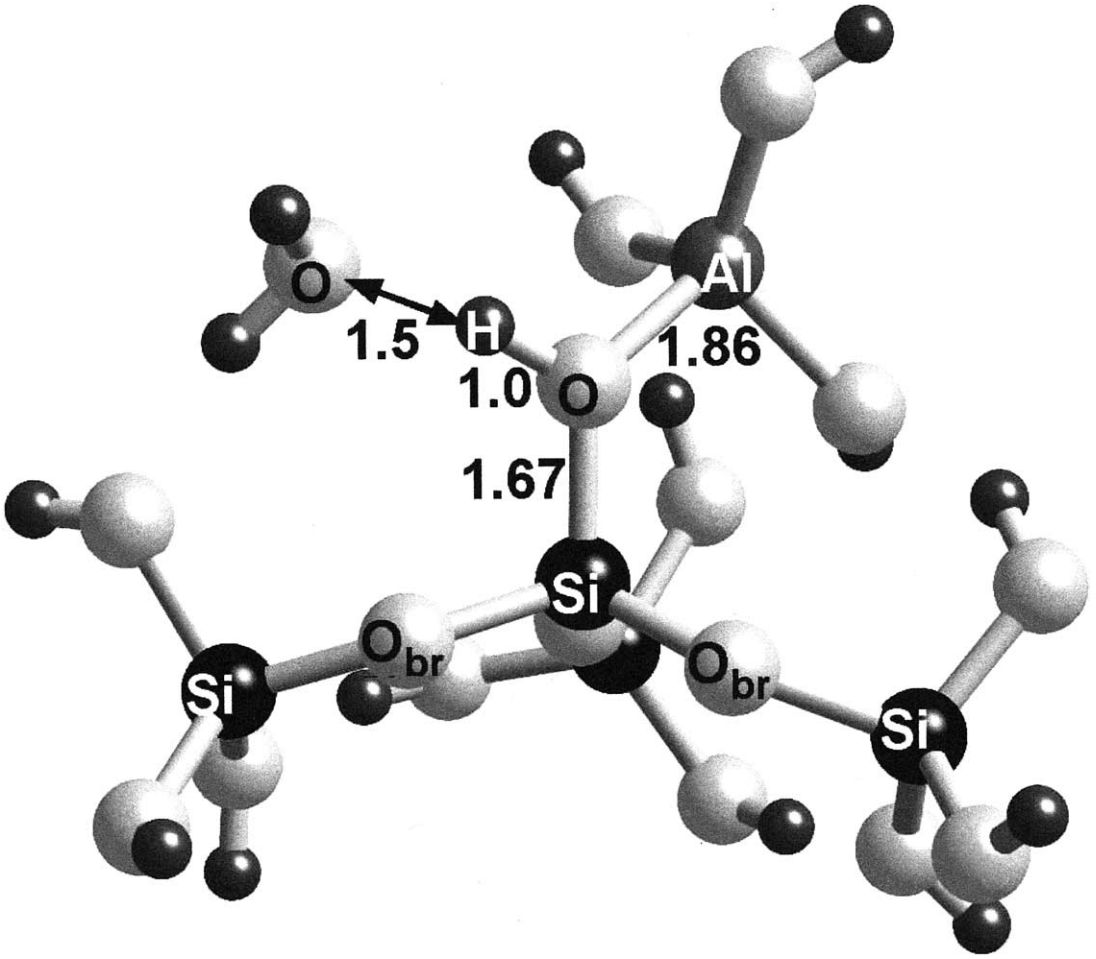

Fig. 2. Q^4 Si with protonated Si-(OH)-Al linkage suggested by Kohn et al. (1992) with H_2O molecule H-bonded at 1.5 Å to the H atom in the Si-(OH)-Al linkage. Note that a variety of similar configurations (both Al- and Si-centered) were modeled in this study as well (Tables 1–4).

configuration is 57 or 64 ppm depending on whether or not H-bonding is included (Table 4).

Conclusive interpretations are difficult to achieve regarding the $\delta_{iso}{}^1H$ chemical shifts. The $\delta_{iso}{}^1H$ in the Q^3 T(OH) silanol and aluminol all have calculated $\delta_{iso}{}^1H$ values comparable to experiment (Table 5). The $H^+(Si_4)Al$ and $H^+(Si_3Al)Si$ models result in calculated $\delta_{iso}{}^1H$ values close to those observed in hydrous albite glass (Zeng et al., 1999). We note that these two model clusters actually model the same species in the glass (i.e., Q^4 Si-[OH]-Q^4 Al). Thus, it is not clear why these two structures would give rise to the two separate peaks observed. The change is likely due to the different T-O-T angles in these two model clusters. The addition of H_2O to the T-(OH)-T clusters increases the predicted values significantly enough to eliminate the agreement with experiment (Table 5). In this case, the effect of H-bonding is known from experiment and will increase the $\delta_{iso}{}^1H$ by 3 to 4 ppm (Zeng et al., 1999).

We conclude that the Q^3 T(OH) models best explain the ^1H-NMR data because the isolated and H-bonded silanol and aluminol values are all close to observed peaks. If these structures were to occur in hydrous albite glass, this would imply depolymerization of Si-O-Si and Si-O-Al linkages. However, the $H^+(Si_4)Al$ and $H^+(Si_3Al)Si$ models also have calculated $\delta_{iso}{}^1H$ values consistent with experiment (Table 5). One way to satisfy both of these predictions is to have both Q^3 SiOH and $H^+(Si_4)Al$ present in hydrous albite glass (Xu et al., 1998; Oglesby and Stebbins, 2000; Schmidt et al., 2000). This implies that the stronger Si-O-Si linkages hydrolyze and the weaker Si-O-Al linkages do not. This is contrary to the hypothesis suggested in Sykes and Kubicki (1993), which focused on hydrolysis of the weaker and more hydrophilic of these linkages, namely Si-O-Al.

3.5. Comparison of Model Results to Hydrous Albite Glass Vibrational Spectra

In Sykes and Kubicki (1993), we argued that the Kohn et al. (1992) model did not adequately address the changes observed in the vibrational spectra of hydrous albite melts as represented in the quenched glasses. A shoulder near 900 cm^{-1} was observed in the hydrous glass spectrum that was not observed in the anhydrous glass spectra (Mysen et al., 1980; McMillan et al., 1983; Mysen and Virgo, 1986; Silver and Stolper, 1989). Hence, model vibrational frequencies were also calculated in

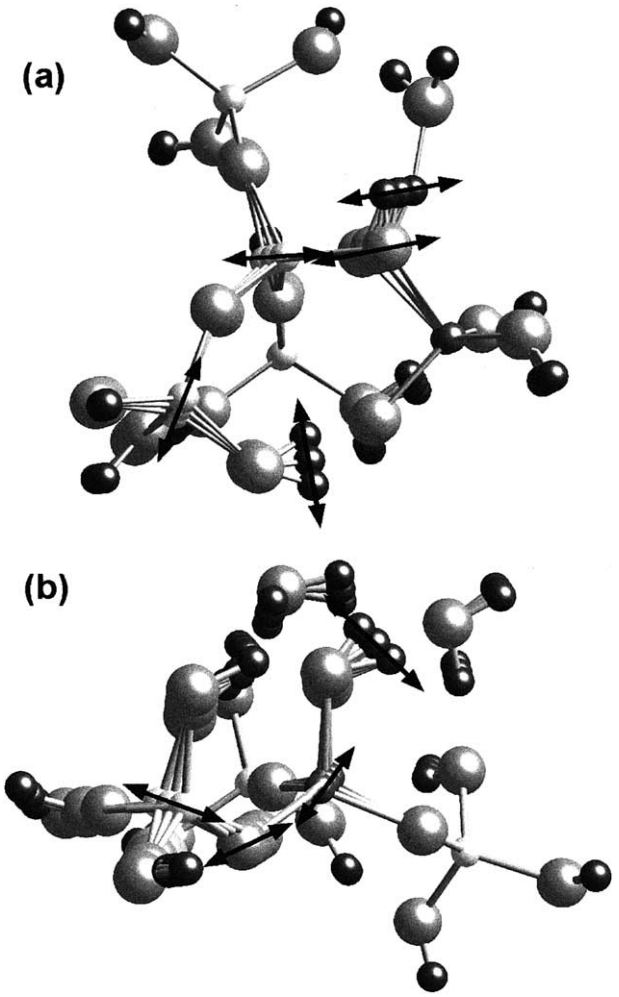

Fig. 3. Depiction of the vibrational modes calculated at (a) 888 cm^{-1} for the Kohn et al. (1992) model and at (b) 790 cm^{-1} for the Sykes and Kubicki (1993) model. The arrows and multiple overlapping atoms represent the displacements involved with each mode.

this study to verify that the T-(OH)-T configuration could reproduce the observed frequency changes. In each model cluster, there will be 3*N*-6 vibrational frequencies where *N* is the number of atoms in the system. We focus on vibrations near 900 cm^{-1} that are associated with the $(OH)^-$ group relevant to the dissolution of H_2O (i.e., T-[OH]-T and Q^3 T-[OH]). In addition, we require that each mode be IR- and Raman-active, because the 900 cm^{-1} shoulder was observed in both types of spectra.

In each model pictured in Figure 3, there is one vibrational mode that satisfies the above criteria. The displacements of the vibrational modes are represented in the Figure 3 by arrows. The involvement of numerous heavy atoms in each mode ensures that any frequency shift generated by isotopic substitution of D for H will be small (Mysen and Virgo, 1986). Although the computed frequencies in each case were scaled by 0.89, this scaling was justified by previous studies showing consistent agreement with experiment when this correction is applied (Kubicki and Sykes, 1993; Sykes and Kubicki, 1996). As can be seen in Figure 3, the T-(OH)-T model of Kohn et al. (1992) produces a vibrational frequency of 888 cm^{-1} that agrees with experiment within the accuracy of resolving the 900 cm^{-1} shoulder. Conversely, the Q^3 Al-(OH) stretching mode predicted by the model of Sykes and Kubicki (1993) predicts a frequency of 790 cm^{-1} that is significantly less than the observed peak.

4. DISCUSSION

The conclusions reached in this paper, based on a more complete experimental data set and model results than previously available, are contrary to our earlier papers (Sykes and Kubicki, 1993; Sykes et al., 1997). We conclude that the Si-(OH)-Al configuration is a preferable explanation of the H_2O dissolution mechanism in fully-polymerized Na-aluminosilicate melts because the $\delta_{iso}{}^{17}O$ values for Al-(OH) do not coincide with the experimental values with or without H-bonding (Table 3). Hence, unless there is an undetected ^{17}O NMR peak between −20 and +5 ppm that corresponds to oxygen in an Al-(OH) group, then we rule out Q^3 Al-(OH) species based on the ^{17}O NMR spectra. Combined with the observation that H_2O depolymerizes SiO_2 melts (Stolen and Walrafen, 1976) and our explanation of the $\delta_{iso}{}^1H$-NMR, we suggest that depolymerization of Si-O-Si groups does occur but Si-O-Al linkages become Si-(OH)-Al in the *glass*. A similar argument can be applied to the work of Keppler and coworkers (e.g., Zotov and Keppler, 1998) who inferred depolymerization of Na-*aluminosilicate* melts from observations of depolymerization in Na-*silicate* glasses.

Zeng and coworkers performed ^1H-^{29}Si CP-MAS NMR (Zeng et al., 2000) and TRAPDOR NMR studies (Zeng et al., 1999) that led them to suggest that water dissolution depolymerized Na-aluminosilicate melts. Based on the ^1H-^{29}Si CP-MAS NMR, Zeng et al. (2000) suggested that SiOH groups may be present in the glass. Oglesby and Stebbins (2000) reached a similar conclusion in their ^1H-^{29}Si CP-MAS NMR investigation of hydrated aluminosilicate glasses. Evidence for the presence of Q^3 AlOH groups was less clear (Zeng et al., 2000). For example, a peak maximum at 1.5 ppm peak in ^1H MAS NMR spectra was assigned to Q^3 Al-(OH) groups by Zeng et al. (1999). Although the $Na^+(Si_3)Al(OH) + 2H_2O$ cluster has a calculated $\delta_{iso}{}^1H = 1.7$ ppm consistent with the assignment of Zeng et al. (1999), the value calculated for $H^+(Si_4)Al$ of 3.3 ppm is also reasonably close to the observed 1.5 ppm peak (Table 5). Note, however, that when H_2O is H-bonded to this Si-(OH)-Al, $\delta_{iso}{}^1H > 10$ ppm (Table 5) suggesting that H-bonding to Si-(OH)-Al does not occur. The same model provides better agreement between calculations and experiment when H_2O is not H-bonded to Si-(OH)-Al for the $\delta_{iso}{}^{17}O$ values (Table 3). Consequently, our results suggest that molecular H_2O associates with Si-OH but not as much with Si-(OH)-Al.

Four questions remain regarding comparisons of observed NMR spectra and model results.

1) Why are the calculated ^{27}Al C_q values for Al-(OH)-Si linkages in agreement with experiments on zeolites but not with spectra of hydrous albitic glasses?
2) How can the observed ^{23}Na NMR spectra be explained?

3) Will T-(OH)-T linkages that are apparently stable in hydrous Na-aluminosilicate glasses be stable in hydrous Na-aluminosilicate melts?
4) Can the protonated bridging oxygen structure explain the large decrease in viscosity of hydrous albitic melts compared to anhydrous melts?

Theoretical calculations predict a significant increase in ^{27}Al C_q with protonation of the Al-O-Si linkage to form Al-(OH)-Si (from 6 to 16 MHz; Sykes et al., 1997; J. A. Tossell, personal communication). NMR spectra of protonated linkages in zeolites also indicate an increase in ^{27}Al C_q from 6 to 16 MHz (Hunger and Horvath, 1995). In contrast, C_q values derived from the NMR spectra of hydrous aluminosilicate glasses indicate a decrease in C_q with protonation (Kohn et al., 1992; Liu et al., 2002). Liu et al. (2002) suggest that perhaps the size of the aluminosilicate clusters may not be sufficiently large to account for all of the contributions to the C_q and that this discrepancy maybe an artifact of the theoretical method. However, there is excellent agreement between calculated and experimentally-derived C_qs for all nuclei in simple alcohol and amide complexes (Ludwig et al., 1995; Farrar et al., 1999). Furthermore, from the current work and in Kubicki and Toplis (2002), ^{27}Al C_q values generally seem to be overestimated by ≈1 MHz wherever comparisons are unambiguous, significantly less than the predicted change of 10 MHz with protonation of the bridging oxygen. Further work will be necessary to resolve this discrepancy. A calculation on a Q^4 Si-(OH)-Q^4 Al model cluster may be necessary to test this explanation.

The second question revolves around Na^+, the remaining ion of interest in Na-aluminosilicate glasses that was not covered in this study. Kohn and coworkers (Kohn et al., 1992, 1998) have observed significant changes in the NMR spectra of ^{23}Na in hydrous Na-aluminosilicate glasses and suggested that Na^+ plays a role in dissolution of H_2O. If a species such as Si-(OH)-Al forms, then a hydroxide ion is also likely to form. A candidate for this species is NaOH (i.e., $NaAlSi_3O_8 + H_2O \rightarrow Al[OH]Si_3O_7 + NaOH$). We have not addressed this issue here for a number of reasons. First, modeling the Na^+ environment in a glass requires a large cluster to account for all the bonds to the Na^+ ion. Second, this issue has been addressed before (Tossell, 1999), and it may be difficult to distinguish among several possibilities of Na^+ speciation based on MO calculations (e.g., NaOH vs. Na-OH_2). Charge-balancing cations such as Na^+ can also affect calculated δ^{17}O values (Kubicki and Toplis, 2002), so inadequate representation of the Na^+ environment may be causing inaccuracies in some of our model δ^{17}O values.

The third issue to be resolved is whether or not the T-(OH)-T linkages are stable at melt temperatures or whether they form upon quenching. To estimate the energy required to break this type of linkage, the optimized structures of $H^+(Si_3Al)Si + H_2O$ (Fig. 2) and $H^+(Si_4)Al + H_2O$ were subjected to constrained energy minimizations as the central T-O distance was lengthened in the T-(OH)-T linkages (Fig. 4). With Si—O values of 2.0, 2.25, 2.5, 3.0, and 3.5 Å, the computed energy at the B3LYP/6-311+G(d,p)//HF/3-21G(d,p) level gradually increased by +56 at 2.5 Å for $H^+(Si_3Al)Si + H_2O$, then began to decrease beyond this distance. For $H^+(Si_4)Al + H_2O$, the energy increased by +82 kJ/mol at Al—O = 4.0 Å (Fig. 4a) and the calculation was not carried further. (The 4.0 Å distance is much longer than any known Si-O or Al-O bonds even for phases where Si and Al are in octahedral coordination; hence, we consider the T-O bond to be "broken" beyond this point.) In both cases, the calculated energy required to break the T-(OH)-T linkage is significantly less than that calculated with the same methods for the model clusters $Na^+([Si_3Al]Si)$ and $Na^+([Si_4]Al)$ (+162 and +132 kJ/mol, respectively). The relatively small energies predicted to break these T-(OH)-T linkages are comparable to experimentally-derived activation energies for viscous flow in hydrous albite melts. For example, the activation energy for viscous flow decreases from 210 to 165 kJ/mol for melts with 0.65 wt.% and 2.8 wt.% water, respectively (Holtz et al., 1999). Activation energies reported by Romano et al. (2001) are considerably higher but decrease from dry to hydrous melt compositions; 488 kJ/mol for dry albite melt and 329 kJ/mol for a melt with 3 wt.% water.

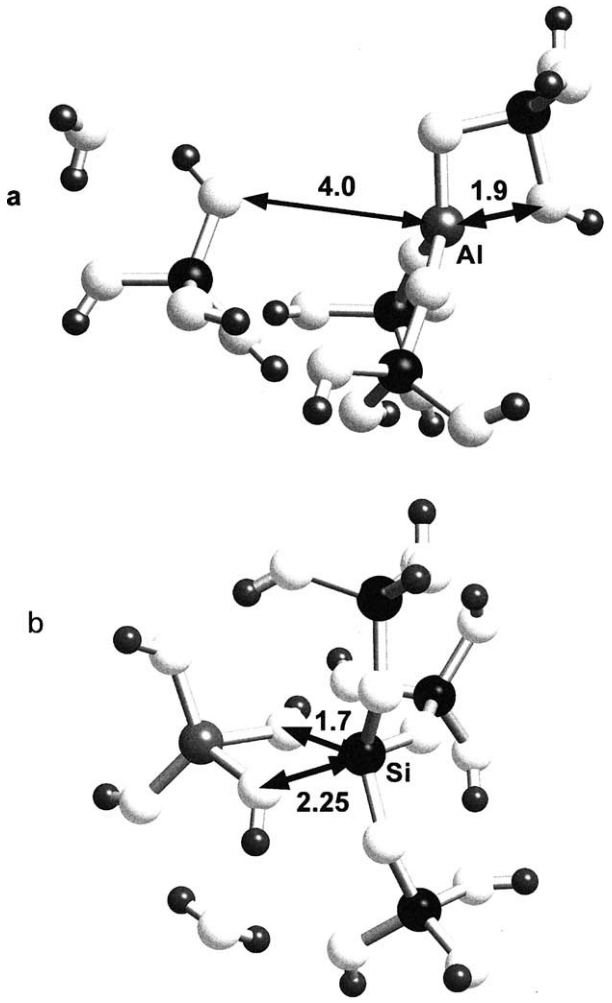

Fig. 4. Models of steps along the constrained optimization sequences for breaking (a) Si-(OH)-Al and (b) Al-(OH)-Si linkages. Note that in (a) the central Al atom takes on a trigonal planar configuration. An OH group from an attached $OSi(OH)_3$ group attempts to approach the central Al, but the interatomic distance (≈1.9 Å) is too large for a tetrahedral Al-O bond. In (b), the leaving OH group is at 2.25 Å, but a second OH from this same $Si(OH)_4$ tetrahedron has already formed a new bond to main the tetrahedral coordination of the central Si atom.

For the series of constrained T-O distance energy minimizations in $H^+(Si_4)Al + H_2O$, the T-O bond re-formed and the model adopted a structure close to the original energy minimized structure even for Si-O and Al-O bonds stretched to distances up to 2.25 and 4.0 Å, respectively. Although viscous flow probably requires the breaking of T-O bonds in the melt, the driving force for either Si or Al to maintain tetrahedral coordination prompts reformation of the Si-(OH)-Al linkage as a likely quench feature in the glass.

As such, H_2O and F^- have a similar influence on the viscosity of aluminosilicate liquids (Dingwell and Mysen, 1985; Dingwell, 1987; Baker and Vaillancourt, 1995; Dingwell and Hess, 1998; Romano et al., 2001), but the different structures observed in their corresponding glasses (Kohn et al., 1992; Zeng and Stebbins, 2000) may arise because reformation of the T-O-T linkage upon quenching is not energetically favorable when F^- is bonded to Al.

High-temperature Raman experiments on hydrous Na-aluminosilicate glasses (e.g., Shen and Keppler, 1995, 1997) could be useful in further study of this issue. Different melt and glass structures could help explain this earlier data that shows complete miscibility between $NaAlSi_3O_8$ and H_2O at high temperatures. If dissolving H_2O in $NaAlSi_3O_8$ melts did not cause some depolymerization, one would expect to see a two-phase region between these two liquids because aluminosilicate polymers would have to depolymerize to dissolve into the H_2O bearing phase. An H_2O dissolution mechanism that does not depolymerize the melt is not compatible with complete miscibility in this system.

Acknowledgments—We thank Yun Liu (SUNY Stony Brook) for discussion of his work in progress. This work supported by The Office of Naval Research and The National Science Foundation. Computational facilities were provided by the DoD High-Performance Computing Initiative through the Aeronautical Systems Center (Dayton, OH) and the Space and Naval Warfare Systems Center (San Diego, CA) and by the Center for Materials Simulation at PSU.

Associate editor: C. Romano

REFERENCES

Baker D. R. and Vaillancourt J. (1995) The low viscosities of $F+H_2O$-bearing granitic melts and implications for melt extraction and transport. *Earth Planet. Sci. Lett.* **132,** 199–211.

Burnham C. W. (1979) The importance of volatile constituents. In *The Evolution of Igneous Rocks* (ed. H. S. Yoder), pp. 439–482. Princeton University Press, Princeton, NJ.

Casanovas J., Pacchioni G., and Illas F. (1999) Si-29 solid state NMR of hydroxyl groups in silica from first principle calculations. *Mater. Sci. Eng. B: Solid State Mater. Adv. Technol.* **B68,** 16–21.

Chuang I. S., Kinney D. R., and Maciel G. E. (1993) Interior hydroxyls of the silica-gel system as studied by Si-29 CP-MAS NMR-spectroscopy. *J. Am. Chem. Soc.* **115,** 8695–8705.

Clark T. M. and Grandinetti P. J. (2003) Dependence of bridging oxygen ^{17}O quadrupolar coupling parameters on Si-O distance and Si-O-Si angle. *J. Phys: Condens. Matter* **15,** S2387–S2395.

Cong X. D. and Kirkpatrick R. J. (1996) O-17 MAS NMR investigation of the structure of calcium silicate hydrate gel. *J. Am. Ceram. Soc.* **79,** 1585–1592.

Dingwell D. B. (1987) Melt viscosities in the system $NaAlSi_3O_8$-H_2O-F_2O^{-1}. *Geochem. Soc. Spec. Pub.* **1,** 423–433.

Dingwell D. B. and Mysen B. O. (1985) Effects of fluorine and water on the viscosity of albite melt at high pressure: A preliminary investigation. *Earth Planet. Sci. Lett.* **74,** 266–274.

Dingwell D. B. and Hess K. U. (1998) Melt viscosities in the system Na-Fe-Si-O-F-Cl: Contrasting effect of F and Cl in alkaline melts. *Am. Mineral.* **83,** 1016–1021.

Dirken P. J., Kohn S. C., Smith M. E., and van Eck E. R. H. (1997) Complete resolution of Si-O-Si and Si-O-Al fragments in an aluminosilicate glass by ^{17}O multiple quantum magic angle spinning NMR spectroscopy. *Chem. Phys. Lett.* **266,** 568–574.

Farnan I., Kohn S. C., and Dupree R. (1987) A study of the structural role of water in hydrous silica glass using cross-polarization magic angle spinning NMR. *Geochim. Cosomochim. Acta* **51,** 2869–2874.

Farrar T. C., Wendt M. A., and Zeidler M. D. (1999) Oxygen-17-induced proton relaxation rates for alcohols and alcohol solutions. *J. Brazil Chem. Soc.* **10,** 321–325.

Felipe M., Xiao Y., and Kubicki J. D. (2001) Molecular orbital modeling and transition state theory in the geosciences. *Rev. Mineral. Geochem.* **42,** 485–531.

Frisch M. J, et al. (1998) *Gaussian 98, Revision A.7*. Gaussian, Inc., Pittsburgh, PA.

Grandinetti P. J., Baltisberger J. H., Farnan I., Stebbins J. F., Werner U., and Pines A.(1995) Solid-State O-17 Magic-Angle and Dynamic-Angle Spinning Nmr-Study of the Sio2 Polymorph Coesite. *J. Phys. Chem.* **99,** 12341–12348.

Holtz F., Roux J., Ohlhorst S., Behrens H., and Schulze F. (1999) The effects of silica and water on the viscosity of hydrous quartzofeldspathic melts. *Am. Mineral.* **84,** 27–36.

Hunger M. and Horvath T. (1995) Multinuclear solid-state NMR study of the local structure of SiOHAl groups and their interaction with probe-molecules in dehydrated faujasite, mordenite and zeolite ZSM-5. *Berichte Bunsen-Gesellschaft* **99,** 1316–1320.

Kohn S. C., Dupree R., and Smith M. E. (1989) A multinuclear magnetic resonance study of the structure of hydrous albite glasses. *Geochim. Cosmochim. Acta* **53,** 2925–2935.

Kohn S. C., Dupree R., and Mortuza M. G. (1992) The interaction between water and aluminosilicate magmas. *Chem. Geol.* **96,** 399–409.

Kohn S. C., Smith M. E., Dirken P. J., van Eck E. R. H., Kentgens A. P. M., and Dupree R. (1998) Sodium environments in dry and hydrous albite glasses: Improved ^{23}Na solid state NMR data and their implications for water dissolution mechanisms. *Geochim. Cosmochim. Acta* **62,** 79–87.

Kohn S. C. (2000) The dissolution mechanisms of water in silicate melts; a synthesis of recent data. *Mineral. Mag.* **64,** 389–408.

Kubicki J. D. and Sykes D. (1993) Molecular orbital calculations of vibrations in three-membered aluminosilicate rings. *Phys. Chem. Miner.* **19,** 381–391.

Kubicki J. D. and Toplis M. J. (2002) Molecular orbital calculations on aluminosilicate tricluster molecules: Implications for the structure of aluminosilicate glasses. *Am. Mineral.* **87,** 668–678.

Lee S. K. and Stebbins J. F. (2000) The structure of aluminosilicate glasses: High-resolution ^{17}O and ^{27}Al MAS and 3QMAS NMR study. *J. Phys. Chem. B* **104,** 4091–4100.

Liu Y., Nekvasil H., and Long H. (2002) In support of a Si-O-Si depolymerisation model for water dissolving in albite glasses: Information from ab initio NMR calculations. *Geochim. Cosmochim. Acta* **66,** 4149–4163.

Ludwig R., Weinhold F., and Farrar T. C. (1995) Experimental and theoretical determination of the temperature dependence of the deuteron and oxygen quadrupole coupling constants in liquid water. *J. Chem. Phys.* **103,** 6941–6950.

Maekawa H., Saito T., and Yokokawa T. (1998) Water in silicate glass: O-17 NMR of hydrous silica, albite, and $Na_2Si_4O_9$ glasses. *J. Phys. Chem. B* **102,** 7523–7529.

McMillan P. F., Jakobsson S., Holloway J. R., and Silver L. A. (1983) A note on the Raman spectra of water-bearing albite glasses. *Geochim. Cosmochim. Acta* **47,** 1937–1943.

Murdoch J. B., Stebbins J. F., and Carmichael I. S. E. (1985) High-resolution ^{29}Si NMR study of silicate and aluminosilicate glasses: The effect of network modifying cations. *Am. Mineral.* **70,** 332–343.

Mysen B. O. and Virgo D. (1986) Volatiles in silicate melts at high pressure and temperature. 2. Water in melts along the join $NaAlO_2$-SiO_2 and a comparison of solubility mechanisms of water and fluorine *Chem. Geol.* **57,** 333–358.

Mysen B. O., Virgo D., Harrison W., and Scarfe C. (1980) Solubility mechanisms of H_2O in silicate melts at high pressures and temperatures: A Raman spectroscopic study. *Am. Mineral.* **65,** 900–914.

Oestrike R., Yang W. H., Kirkpatrick R. J., Hervig R. L., Navrotsky A., and Montez B. (1987) High-resolution ^{23}Na, ^{27}Al, ^{29}Si NMR spectroscopy of framework aluminosilicate glasses. *Geochim. Cosmochim. Acta* **51,** 2199–2209.

Oglesby J. V. and Stebbins J. F. (2000) 29Si CPMAS NMR investigations of silanol-group minerals and hydrous aluminosilicate glasses. *Amer. Mineralogist* **85,** 722–731.

Pople J. A., Schlegel H. B., Krishnan R., Defrees D. J., Binkley J. S., Frisch M. J., Whiteside R. A., Hout R. F., and Hehre W. J. (1981) Molecular orbital studies of vibrational frequencies. *Int. J. Quant. Chem: Quant. Chem. Symp.* **15,** 269–278.

Pyykkö P. (1992) The nuclear quadrupole moments of the first 20 elements: High-precision calculations on atoms and small molecules. *Z. Natur.* **47a,** 189–196.

Romano C., Poe B. T., Mincione V., Hess K. U., and Dingwell D. B. (2001) The viscosities of dry and hydrous $XAlSi_3O_8$ (X=Li, Na, K, $Ca_{0.5}$, $Mg_{0.5}$) melts. *Chem. Geol.* **174,** 115–132.

Schmidt B. C., Riemer T., Kohn S. C., Behrens H., and Dupree R. (2000) Different water solubility mechanisms in hydrous glasses along the Qz-Abjoin: Evidence from NMR spectroscopy. *Geochim. Cosmochim. Acta,* **64,** 513–526.

Shen A. H. and Keppler H. (1995) Infrared spectroscopy of hydrous silicate melts to 1000 degrees C and 10 kbar: Direct observation of H_2O speciation in a diamond-anvil cell. *Am. Mineral.* **80,** 1335–1338.

Shen A. H. and Keppler H. (1997) Direct observation of complete miscibility the albite-H_2O system. *Nature* **385,** 710–712.

Silver L. and Stolper E. M. (1989) Water in albitic glasses. *J. Petrol.* **30,** 667–709.

Stolen R. and Walrafen G. (1976) Water and its relation to broken bond defects in fused silica. *J. Chem. Phys.* **64,** 2623–2631.

Sykes D. G. and Kubicki J. D. (1993) A model for H_2O solubility mechanisms in albite melts from infrared spectroscopy and molecular orbital calculations. *Geochim. Cosmochim. Acta* **57,** 1039–1052.

Sykes D. and Kubicki J. D. (1996) Four-membered rings in silica and aluminosilicate glasses. *Am. Mineral.* **81,** 265–272.

Sykes D., Kubicki J. D., and Farrar T. C. (1997) Molecular orbital calculation of ^{27}Al and ^{29}Si NMR parameters in Q^3 and Q^4 aluminosilicate molecules and implications for the interpretation of hydrous aluminosilicate glass NMR spectra. *J. Phys. Chem.* **101,** 2715–2722.

Tossell J. A. (1999) Quantum mechanical calculation of ^{23}Na NMR shieldings in silicates and aluminosilicates. *Phys. Chem. Miner.* **27,** 70–80.

van Eck E. R. H., Smith M. E., and Kohn S. C. (1999) Observation of hydroxyl groups by O-17 solid-state multiple quantum MAS NMR in sol-gel-produced silica. *Solid State Nucl. Magn. Reson.* **15,** 181–188.

Walter T. H., Turner G. L., and Oldfield E. (1988) Oxygen-17 cross-polarization NMR spectroscopy of inorganic solids. *J. Magn. Reson.* **76,** 106–120.

Xu Z. and Stebbins J. F. (1998) Oxygen sites in the zeolite stilbite: A comparison of static, MAS, VAS, DAS and triple quantum MAS NMR techniques. *Solid State Nucl. Magn. Reson.* **11,** 243–251.

Xu Z., Maekawa H., Oglesby J. V., and Stebbins J. F. (1998) Oxygen speciation in hydrous silicate glasses: An oxygen-17 NMR study. *J. Am. Chem. Soc.* **120,** 9894–9901.

Xue X. and Kanzaki M. (1998) Correlations between ^{29}Si, ^{17}O and ^{1}H NMR properties and local structures in silicates: *Ab initio* calculation. *Phys. Chem. Miner.* **26,** 14–30.

Xue X. and Kanzaki M. (1999) NMR characteristics of possible oxygen sites in aluminosilicate glasses and melts: An ab initio study. *J. Phys. Chem. B* **103,** 10816–10830.

Zeng Q. and Stebbins J. F. (2000) Fluoride sites in aluminosilicate glasses: High-resolution ^{19}F NMR results. *Am. Mineral.* **85,** 863–867.

Zeng Q., Nekvasil H., and Grey C. P. (1999) Proton environments in hydrous aluminosilicate glasses: A ^{1}H MAS, $^{1}H/^{27}Al$, and $^{1}H/^{23}Na$ TRAPDOR NMR study. *J. Phys. Chem. B* **103,** 7406–7415.

Zeng Q., Nekvasil H., and Grey C. P. (2000) In support of a depolymerization model for water in sodium aluminosilicate glasses: Information from NMR spectroscopy. *Geochim. Cosmochim. Acta* **64,** 883–896.

Zotov N. and Keppler H. (1998) The influence of water on the structure of hydrous sodium tetrasilicate glasses. *Am. Mineral.* **83,** 823–834.